IARJSET ISSN (O) 2393-8021, ISSN (P) 2394-1588

International Advanced Research Journal in Science, Engineering and Technology

ISO 3297:2007 Certified ⁜ Impact Factor 8.066 ⁜ Peer-reviewed / Refereed journal ⁜ Vol. 10, Issue 7, July 2023

DOI: 10.17148/IARJSET.2023.10710

NATURAL GAS PRODUCTION FIRED COMBINED CYCLE POWER PLANT DEVELOPMENT OF TRI-GENERATION ENERGY, COOLING AND SAFE WATER BY RECOVERING HEAT GENERATED: A TECHNICAL AND ECONOMIC EVALUATION.

NNADIKWE JOHNSON[1], IKOKO IKECHUKWU[2], SAMUEL H. KWELLE[3]

IMO STATE UNIVERSITY[1]

NETCODIETSMANN[2]

FIRST INDEPENDENT POWER LIMITED[3]

Abstract: One of the most effective methods for maximizing the use of available energy is trigeneration. This research study examines the use of waste heat (flue gases) released by the Afam V1 gas turbine power plant for the simultaneous production of electricity, clean water and cooling using a single stage vapour absorption chiller (VAC) by combining steam with a Rankine cycle and a heat recovery steam generator (HRSG). The trigeneration system's main source of energy comes from the flue gases released during the gas turbine power cycle. The thermal energy recovered from the steam cycle's condenser and the extra heat present in the flue gases are used to power desalination and cooling cycles that are tailored to the villas' specific cooling requirements. The trigeneration system's financial and environmental advantages in terms of savings in expenses and a decrease in carbon emissions were examined. The trigeneration system achieves energy efficiency of around 82%-85% as opposed to combined cycles at 50%-52%. Implementing a waste thermal recovery tri-generation system reduces standardized carbon dioxide emission per MWh by 51.5%. The payback period for the trigeneration system is 1.38 years, and its total net present value for the duration of the project is $66 million.

Keywords: air gap membrane distillation, tri-generation, techno-economic, waste heat, steam cycle, absorption chillers, flue gases.

I. INTRODUCTION

Among the many potential technological integration practices, tri-generation produces three distinct outputs from a single input of energy. Adding heat-driven cooling and desalination cycles to a combined heat and power cycle (CHP) would make it a poly-generation system. Poly-generation cycles maximize energy usage while simultaneously decreasing GHG emissions [1–5]. The term "combined cooling, heat, and power" (CCHP) refers to an expanded form of CHP intended for the efficient central generation of cooling, heating, and electricity at a large scale [6]. Power stations in the MENA area often incorporate desalination facilities to recover waste heat and provide potable water for local use. However, tri-generation models that produce cooling, clean water, and power (CCCWP) would be more advantageous in terms of energy savings and economics because decentralized air conditioning systems throughout the region account for greatest power usage.

Several researchers have looked into CCHP setups that include absorption, adsorption, or desiccant chillers in addition to gas turbines, steam turbines, and organic Rankine cycles. In order to provide cooling, hot water, and power, Ahmadi et al. [7] performed extensive thermodynamic modelling of CCHP. Single-stage absorption chiller for cooling, hot water via heat recovery, and combined gas turbine and organic Rankine cycle power generation make up the modelled system. Tri-generation systems have a 20% higher exergy efficiency than standard CHP, according to the system's energy efficiency and environmental impact analysis. Khaliq [8] modelled a tri-generation system that uses gas turbines to generate electricity, cooling, and heat (process steam). Various pressure to temperature ratios, turbine input temperatures,

IARJSET ISSN (O) 2393-8021, ISSN (P) 2394-1588

International Advanced Research Journal in Science, Engineering and Technology

ISO 3297:2007 Certified ⁜ Impact Factor 8.066 ⁜ Peer-reviewed / Refereed journal ⁜ Vol. 10, Issue 7, July 2023

DOI: 10.17148/IARJSET.2023.10710

process heat pressures, and evaporator temperatures of the absorption chiller are considered in order to determine the system's performance. Tri-generation systems that generate electricity using gas turbine and steam turbine cycles were the subject of extensive thermodynamic modelling and simulation by Ahmadi et al. [9]. To cool the building, a steam-powered absorption chiller draws heat from the building's low-pressure steam supply, which comes from a heat recovery steam generator (HRSG). Financial benefits inspired the development of many designs for a tri-generation system based on internal combustion (IC) engines used for combined heat and power (CCHP). Temir and Bilge [10] looked at the efficacy of tri-generational systems, which use a combination of absorption cooling using saturated steam from the boiler, heat from processing recovery from exhaust outlets, and power generation via reciprocating engines. Using reciprocating engines with internal combustion, absorption chillers, and heat recovery devices, Huangfu et al. [5] evaluated the efficiency of micro-scale CCHP for residential and light commercial use. The payback time, according to energy and cost studies, is only 2.97 years. To reduce primary energy consumption by 37% compared to traditional power and cooling systems, Sun [11] presented a combined production cycle of electricity by gas engine and cooling by absorption chiller, with a payback return of 4.52 years.

Few researchers have looked into tri- or poly-generation systems that combine desalination processes to produce pure water. Hussain [12] created a tri-generation system for the concurrent creation of cooling, clean water, and power, and he analysed several technologies for providing both of these resources. To maximise fuel efficiency, the system has been fine-tuned. The most cost-effective solution is a hybrid system that combines a reverse osmosis water purification system with an absorption chiller and a gas turbine power cycle. For CCCWP purposes, Calise et al. [13] modelled a solar-powered three-generation system. The hybrid photovoltaic-thermal (PVT) collectors, vapour absorption chiller, and multi-effect desalination unit all work together to generate cooling, desalination, and electricity. We did transient simulations with varying operating and design factors and optimised them for energy efficiency and cost effectiveness. This study looks at a tri-generational system that includes a combined cooling, clean water, and power cycle (CCCWP) using membrane distillation technology for clean water production. A potential thermal driven desalination technique is membrane distillation, which uses low-grade heat energy to produce pure water [14]. In the past, scientists have studied how to best incorporate a membrane distillation system into a cogeneration setting. Using a gas engine for both power and desalination in one cycle, and a vapour compression chiller for both chilling and distillation in another, Liu [15] compared the efficiency of two cogeneration systems. Kullab [16] examined how well various integration configurations of air gap membrane distillation (AGMD) modules performed. In order to maximise the efficiency of a system that generates 20 L/h of distillate flow per module, Burrieza et al. [17] undertook a series of parametric tests on air gap membrane distillation modules.

II. SYNOPSIS OF THE SYSTEM

Figure 1 illustrates the proposed tri-generation system for the efficient use of the waste flue gases released by the Afam VI gas turbine power station located in River's state, Nigeria. The AFAM VI gas turbine power station has a reheat Brayton cycle arrangement. Compressed air at room temperature is sent to the combustion chamber (CC) to create superheated gas. A set of gas turbines coupled by reheat chambers (RH) expand this superheated gas further to generate electricity.

Figure 1A: AfamVI Gas power plant/first independent power Ltd

IARJSET ISSN (O) 2393-8021, ISSN (P) 2394-1588

International Advanced Research Journal in Science, Engineering and Technology

ISO 3297:2007 Certified ⁜ Impact Factor 8.066 ⁜ Peer-reviewed / Refereed journal ⁜ Vol. 10, Issue 7, July 2023

DOI: 10.17148/IARJSET.2023.10710

Figure 1B: Gas turbine in Afam power plant.

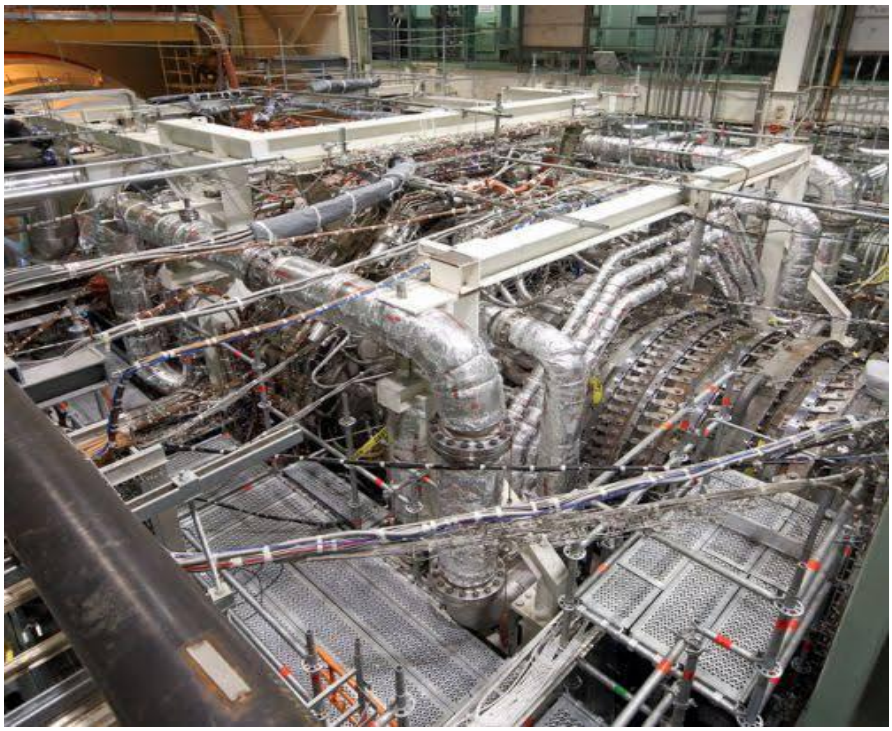

Figure 1C: GE New state of Art of Gas Turbine AFAM VI Power plant

The suggested tri-generation system consists of a steam turbine-driven Rankine cycle, a single stage LiBr/H2O absorption chiller plant, and air gap membrane-based distillation units. Figure 2 depicts the schematic arrangement of a tri-generation system. The hot flue gases released after the turbine's gas expansion are used in the HRSG to produce process steam at a higher pressure and temperature, which is then expanded in a steam turbine to produce power. The steam is subsequently condensed in a seawater heat recovery system. The heat recovered in the heat recovery system powers both the absorption chiller and the membrane distillation system. The feed water pump circulates the condensed steam (feed water) back to the HRSG. The HRSG stack flue gases are used to generate extra hot sea water, which is connected with the supply system and cooling or desalination processes.

IARJSET ISSN (O) 2393-8021, ISSN (P) 2394-1588

International Advanced Research Journal in Science, Engineering and Technology

ISO 3297:2007 Certified ⁜ Impact Factor 8.066 ⁜ Peer-reviewed / Refereed journal ⁜ Vol. 10, Issue 7, July 2023

DOI: 10.17148/IARJSET.2023.10710

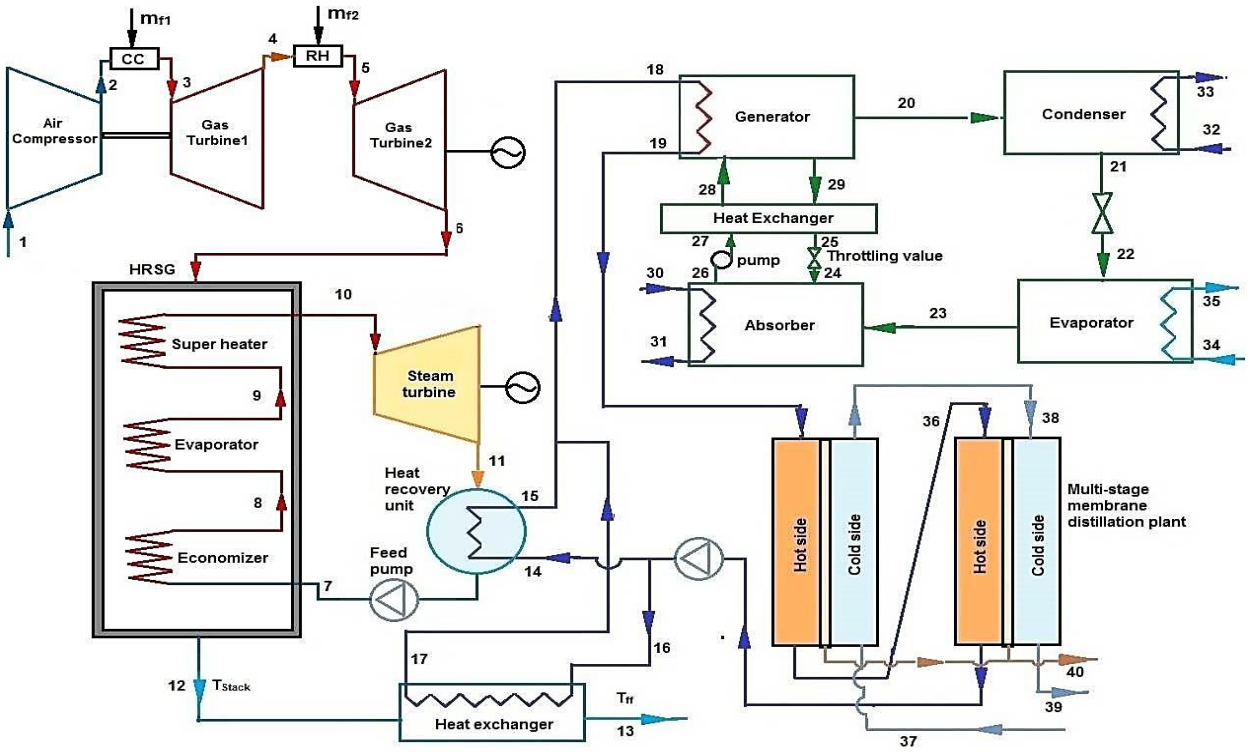

No	Specification	No	Specification
1	Inlet air entering compressor	21	Condensed water exiting condenser
2	Outlet air from compressor	22	Water vapor entering evaporator (VAC)
3	Combustion gases leaving combustion chamber	23	Saturated water entering absorber
4	Hot gases leaving first gas turbine	24	LiBr solution leaving heat exchanger
5	Combustion gases leaving reheat chamber	25	LiBr solution entering absorber
6	Hot flue gases leaving second gas turbine	26	Low pressure LiBr –water mixture
7	Feed water entering HRSG	27	High pressure LiBr- water mixture
8	Hot water leaving economizer	28	Weak solution entering generator
9	Saturated steam leaving evaporator	29	Strong solution leaving generator
10	Super heated steam entering steam turbine	30	Cold sea water entering absorber
11	Expanded steam entering heat recovery unit	31	Sea water leaving absorber
12	Flue gases leaving HRSG	32	Cold sea water entering condenser
13	Flue gases exiting heat exchanger	33	Sea water leaving condenser
14	Sea water entering heat recovery unit	34	Circulation water entering evaporator (VAC)
15	Hot sea water leaving heat recovery unit	35	Chilled water supplied to building
16	Sea water entering heat exchanger	36	Hot sea water supplied to 2nd stage MD
17	Hot sea water exiting heat exchanger	37	Cold sea water supplied to 1st stage MD
18	Hot sea water entering generator	38	Cold sea water supplied to 2nd stage MD
19	Hot sea water to 1st stage membrane distiller (MD)	39	Sea water leaving cold side of MD
20	Water vapor entering condenser	40	Distillate produced in MD

Figure 2. Schematic layout of tri-generation system.

III. MODELLING OF SYSTEMS

3.1. Brayton Cycle

The AFAM gas turbine power plant uses the reheat Brayton design, as seen in Figure 1. The following is a model of the reheat Brayton cycle's energy balance:

At point 1, air at room temperature enters the compressor. The temperature of the air (T2) as it exits the compressor is determined by:

IARJSET ISSN (O) 2393-8021, ISSN (P) 2394-1588

International Advanced Research Journal in Science, Engineering and Technology

ISO 3297:2007 Certified ⁜ Impact Factor 8.066 ⁜ Peer-reviewed / Refereed journal ⁜ Vol. 10, Issue 7, July 2023

DOI: 10.17148/IARJSET.2023.10710

$$\frac{T_2}{T_1} = \left(\frac{Pr_2}{Pr_1}\right)^{\frac{\gamma-1}{\gamma}} \quad (1)$$

where T1 and T2 represent the temperatures of air going into and coming out of the compressor, respectively; Pr1 and Pr2 represent the pressures of air before and after the compression operation; and represents the specific heat ratio. The amount of work done by the compressor may be estimated as follows:

$$W_{\text{Compressor}} = \dot{m}_a C_{p,air}(T_2 - T_1) \quad (2)$$

in which W Compressor is the amount of work performed with the compressor; is the mass flow rate of air; and Cp,air is the amount of heat that may be specifically contained inside air. The compressed air is sent to the CC, which is then used in the combustion chamber (where fuel is also added) to burn the compressed air. The following equations provide the energy balance of the processes in CC:

$$Q_{CC} = \dot{m}_{g,1} C_{p,gas,1} T_3 - \dot{m}_a C_{p,air} T_2 \quad (3)$$

$$Q_{CC} = \dot{m}_{f,1} \cdot LHV \quad (4)$$

where QCC is the heat energy given by the process of combustion chamber; is the total amount of gas exiting the combustion chamber; T3 is the temperature of gas leaving the combustion chamber; and is the rate at which the mass flows of fuel delivered to CC and the lesser temperature-value of fuel. The initially installed gas turbine expands superheated (T3) gas,

$$Q_{gt,1} = \dot{m}_{g,1} C_{p,gas}(T_3 - T_4) \quad (5)$$

where Qgt,1 represents the amount of energy generated by the initially operating gas turbine and T4 represents the temperature of the flue gases exiting the gas turbine. The flue gases released by the initially operating gas turbine are subsequently combusted in the reheating chamber, where energy balance is achieved:

$$Q_{RH} = \dot{m}_{g,2} C_{p,gas,2} T_5 - \dot{m}_{g,1} C_{p,gas,1} T_4 \quad (6)$$

$$Q_{RH} = \dot{m}_{f,2} \cdot LHV \quad (7)$$

The heat energy that is delivered by the reheated chamber is denoted by QRH; the mass of gas that is exiting the reheat section is denoted by; the temperature of gas that is exiting the reheat section is denoted by T5; and the mass flow rate of fuel that is supplied to RH is denoted by. The second gas turbine then performs an expansion using the warmed gas:

$$Q_{gt,2} = \dot{m}_{g,2} C_{p,gas,2}(T_5 - T_6) \quad (8)$$

where T6 is the exhaust temperature of the flue gas that's used to power the tri-generational setup.

3.2. Steam Cycle

3.2.1. Heat Recovery Steam Generator (HRSG)

Using a single pressure HRSG equipped with economizer, evaporator, and super heating subsections, the tri-generation cycle produces super-heated process steam. Figure 3 depicts the HRSG temperature profile. The difference in temperature between the gas and water (at saturation temperature) at the evaporator's inlet is known as the pinch line.

The pinch line is a critical variable in HRSG energy simulations. For the sake of this modelling, we will assume that the pathway temperature corresponding to the economizer's outlet and the evaporator's inlet remains constant. The configuration of the tubes in the economizer circuit determines the incoming air temperature.

IARJSET ISSN (O) 2393-8021, ISSN (P) 2394-1588

International Advanced Research Journal in Science, Engineering and Technology

ISO 3297:2007 Certified ⁜ Impact Factor 8.066 ⁜ Peer-reviewed / Refereed journal ⁜ Vol. 10, Issue 7, July 2023

DOI: 10.17148/IARJSET.2023.10710

Figure 3. T-S diagram for temperature and entropy of Heat Recovery Steam Generator (HRSG).

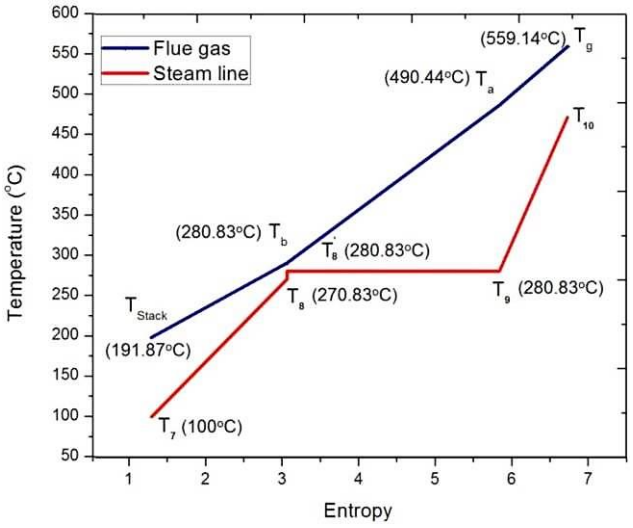

Modelling the energy balance of the HRSG's various portions. It is possible to calculate the evaporator's energy balance by using the temperature differential at the pinch point:

$$\dot{m}_w(h_9 - h_{8'}) = \dot{m}_g C_{P,g}(T_a - T_b) \quad (9)$$

whereby is the total mass rate of flow of the steam production line; is the mass flow rate of hot flue gases; and CP,g is the hot flue gas heat transfer coefficient. h8' and h9 are the saturated water and steam enthalpies, respectively. The boiling point of the gas entering the evaporator is Ta, while the ambient temperature of the gas exiting the evaporator is Tb. The following is the super heater's energy balance:

$$\dot{m}_w(h_{10} - h_9) = \dot{m}_g C_{P,g}(T_6 - T_a) \quad (10)$$

where T6 is the temperature of the hot flue gas entering the HRSG and h10 is the enthalpy of the steam that has become superheated. As an example, consider the economizer's energy balance:

$$\dot{m}_w(h_8 - h_7) = \dot{m}_g C_{P,g}(T_b - T_{Stack}) \quad (11)$$

where TStack is the stack temperature of flue gases exiting the HRSG and h7 and h8 are the temperatures of the heated water at the entry point and exit point of the economizer.

3.2.2. Steam Turbine

A steam turbine is used to expand the high pressure, superheated steam produced in the HRSG to ambient pressure. According to the following formula, energy collected from the turbine (WST):

$$W_{ST} = \dot{m}_w(h_9 - h_{10}) \quad (12)$$

wherein h10 is the concentration of the steam as it exits the turbine.

3.2.3. System of Heat Recovery

Condensed steam from the steam turbine drives the absorption chiller and membrane distillation unit via a heat recovery system that uses steam to transfer heat to sea water. In addition, some of the heat energy lost in the stack flue gases is captured by sea water. It works in tandem with the refrigeration and desalinization module supply chain. For a heat recovery system, the energy balance equation is:

IARJSET ISSN (O) 2393-8021, ISSN (P) 2394-1588

International Advanced Research Journal in Science, Engineering and Technology

ISO 3297:2007 Certified ⁜ Impact Factor 8.066 ⁜ Peer-reviewed / Refereed journal ⁜ Vol. 10, Issue 7, July 2023

DOI: 10.17148/IARJSET.2023.10710

$$Q_{\text{extract}} = \dot{m}_{\text{w}}(h_{11} - h_7) + \dot{m}_{\text{g}} C_{\text{P,g}}(T_{\text{stack}} - T_{\text{ff}}) \quad (13)$$

$$Q_{\text{extract}} = \dot{m}_{\text{SW}} C_{\text{P,SW}}(T_{\text{SW,out}} - T_{\text{SW,in}}) \quad (14)$$

where Qextract is the heat pulled through the steam, h7 is the value of the enthalpy of water exiting the condenser at 100 °C, and Tff is the temperature of the flue gas after the heat exchanger. For sea water, W is the mass flow rate; Specific heat capacity (CP, SW) TSW, in and TSW, out are the sea water temperatures going into and coming out of a heat recovery system, respectively. A heat recovery system's required space is based on:

$$A_{\text{HRS}} = \frac{Q_{\text{extract}}}{U_{\text{HRS}} \times \Delta T_{\text{LMTD}}} \quad (15)$$

wherein TLMTD indicates the logarithmic standard deviation of the temperature difference, UHRS is the total heat transfer coefficient of the heat recovery system, and AHRS is the total surface area of the heat recovery system.

3.3. Absorption Chiller

LiBr/H2O vapour absorption chiller is the absorption chiller taken into account in the tri-generation system.

As illustrated in Figure 4 [18], the system is intended to offer district cooling to several duplex-villas in the area of AFAM IN RIVERS STATE IN NIGERIA. Based on the cooling load needs of villas, the system is optimised. Calculating the vapour absorption chiller's energy balance:

$$Q_{\text{ch}} = \dot{m}_{\text{ac,ch}} C_{\text{p}} \Delta T_{\text{ac,ch}} \quad (16)$$

$$Q_{\text{gen}} = \dot{m}_{\text{SW}} C_{\text{P,SW}} \Delta T_{\text{ac,h}} \quad (17)$$

$$COP_{\text{T}} = \frac{Q_{\text{Ch}}}{Q_{\text{gen}}} \quad (18)$$

in which Qch is the absorption chiller's chilling capacity; Qgen is the heat supplied by the absorption chiller's generator; and are the mass flow rates of chilled water and boiling water flowing within the absorption chiller; Tac,ch is the temperature difference between the chilled-water circuit's inlet and outlet; and Tac,h is the temperature variance between the generator's hot water intake and outlet.

Figure 4. Duplex villa in AFAM V1

IARJSET ISSN (O) 2393-8021, ISSN (P) 2394-1588

International Advanced Research Journal in Science, Engineering and Technology

ISO 3297:2007 Certified ⁜ Impact Factor 8.066 ⁜ Peer-reviewed / Refereed journal ⁜ Vol. 10, Issue 7, July 2023

DOI: 10.17148/IARJSET.2023.10710

3.4. Membrane Distillation

For safe water generation in the tri-generation system, a membrane distillation module with an air gap is proposed. Meffio Technology in Port Harcourt, Nigeria, manufactures the membrane modules under consideration for the investigation. The hot water from the sea exiting the absorption chiller's generator is delivered to a significant number of parallel-connected multi-effect membrane distillation modules. Table 1 shows the technical characteristics of the membrane distillation modules.

Table 1. Membrane module technical specs [16] Technology.

No.	Specification	Value
1	Membrane area	2.8 m^2
2	Porosity (ϕ)	0.8
3	Membrane thickness (b)	0.2 mm
4	Air gap width (L)	1 mm
5	Height of the module	730 mm
6	Width of the module	630 mm
7	Thickness of the module	175 mm

Experimental equations developed through a series of experiments in the Chemical Engineering Department Kinetic Reaction laboratory at Imo State Polytechnic and the Petroleum & Gas Engineering Department, Pulse Plasma Monitoring and Simulation laboratory at Imo State University, as well as the modelling and simulation of porus media laboratory, are used to determine the mass and energy balance of membrane modules [15].

Based on a comprehensive testing campaign, [15] we determined that 1200 kg/h is the ideal selection for the mass flow rate of sea water supplied to the hot and cold side. In this article, we develop the experimental equations for mass and energy flux as a function of porosity, air gap thickness, membrane thickness, and inlet temperatures of hot and cold fluids. The approximations given by these equations are more accurate. [15,16].

$$M_{\text{dis}} = 4.1 \times 10^{-3} \times \frac{1}{[b/(\phi \times \sqrt{T_{\text{MD,H,in}}})] + (L/\sqrt{T_{\text{MD,C,in}}})} \times \ln \frac{(1 - X_{\text{c}})}{(1 - X_{\text{h}})} \qquad (19)$$

wherein Mdis is the hourly distillate production mass per unit membrane surface area, b is the membrane thickness, and L is the air gap distance. The mole fraction of water vapour present at the surface of condensation (Xc) and evaporation (Xh) The AGMD's hot water entry and exit temperatures (TMD, H,in and TMD,H,out) and cold water inlet and outlet temperatures (TMD,C,in and TMD,C,out):

$$X_{\text{c}} = \frac{p_{i,\text{c}}}{P} \qquad (20)$$

$$X_{\text{h}} = \frac{p_{i,\text{h}}}{P} \qquad (21)$$

$$p_{i,\text{c}} = e^{\left(\frac{12.03-4025}{T_{\text{MD,C,in}}+235}\right)} \qquad (22)$$

$$p_{i,\text{h}} = e^{\left(\frac{12.03-4025}{T_{\text{MD,H,in}}+235}\right)} \qquad (23)$$

wherein pi, h and pi, c are the corresponding partial pressures of the vapour on both the cold and hot sides, respectively; P is the overall pressure:

IARJSET ISSN (O) 2393-8021, ISSN (P) 2394-1588

International Advanced Research Journal in Science, Engineering and Technology

ISO 3297:2007 Certified ⁜ Impact Factor 8.066 ⁜ Peer-reviewed / Refereed journal ⁜ Vol. 10, Issue 7, July 2023

DOI: 10.17148/IARJSET.2023.10710

$$E_{MD} = \frac{1.5 \times 10^{-3} \times (T_{MD,H,in} - T_{MD,C,in})}{(b/(\gamma\,\phi\sqrt{T_{MD,H,in}})) + (L/\sqrt{T_{MD,C,in}})} \times \left(1 + 1.41 \times \ln \frac{(1 - X_c)}{(1 - X_h)}\right) \times \frac{b/(\gamma\,\phi\sqrt{T_{MD,H,in}})}{(b/\phi\sqrt{T_{MD,H,in}}) + (L/\sqrt{T_{MD,C,in}})} \quad (24)$$

$$\gamma = \frac{k_{membrane}}{\phi \times k_{air}} \quad (25)$$

Where kair is membrane thermal conductivity of air and k membrane is material specific, is the porosity of the membrane material. To determine how much energy membrane distillation really puts to good use, one can apply the formula:

$$Q_{dis} = M_{dis}\,(\lambda_L) \quad (26)$$

wherein Qdis is the beneficial energy needed to perform vapour evaporation and L denotes the accumulated heat of condensation.

3.5. Energy Conservation

The ratio of useable energy generated by the system to the quantity of energy provided to the system is known as energy conservation. This research examines the efficiency of current gas turbine power plants, coupled cycles, and tri-generation (power, cooling, and desalination):

$$\eta_{GT} = \frac{W_{GT}}{\dot{m}_f \times LHV} \quad (27)$$

$$\eta_{CC} = \frac{W_{GT} + W_{ST}}{\dot{m}_f \times LHV} \quad (28)$$

$$\eta_{Tri} = \frac{W_{GT} + W_{ST} + Q_{ch} + Q_{dis}}{\dot{m}_f \times LHV} \quad (29)$$

wherein WGT and WST represent the work done by the gas turbine and steam turbine respectively, represents the mass flow rate of the fuel, and LHV represents the lower heating value. The energy that is cooled and generated by the absorption chiller is denoted by Qch, whereas the energy that is usable and utilised by the membrane distillation unit is denoted by Qdis.

IV. THE FINDINGS AND DISCUSSION

This section analyses and discusses the thermodynamic calculation and optimization process for a comprehensive tri-generation system for cooling, desalination, and hot water production.

4.1. Brayton Cycle

The AFAM gas turbine power plant provided data and parameters for the computational modelling of the gas turbine cycle [19]. In the AFAM power plant, the reheat-Brayton cycle is optimised to maintain a constant temperature of 1097 K at the inlet conditions of both gas turbines, regardless of air intake temperature.

To obtain 1097 K at the inlet of gas turbines, the pressure ratio and rate of air intake at the compressor unit, as well as the rate of fuel infiltration within the combustion and reheat chambers, were optimised. Table 2 displays the average operational characteristics of a gas turbine. Figure 5 depicts the performance of the Brayton cycle when the air input temperatures are varied.

IARJSET ISSN (O) 2393-8021, ISSN (P) 2394-1588

International Advanced Research Journal in Science, Engineering and Technology

ISO 3297:2007 Certified ⁜ Impact Factor 8.066 ⁜ Peer-reviewed / Refereed journal ⁜ Vol. 10, Issue 7, July 2023

DOI: 10.17148/IARJSET.2023.10710

Table 2. Gas turbine power plant technical details.

Description	Parameters
Gas turbine model (GE-manufacturer)	Model: LM2500 PE, Avio, Italy
Gas turbine inlet temperature	824 °C
Mean intake air temperature	35 °C
Mean exhaust gas flow	64.1 kg/s
Mean exhaust gas temperature	550 °C
Lower Heating Value	47,000 kJ/kg

Figure 5. Gas power cycle performance at varied intake temperatures.

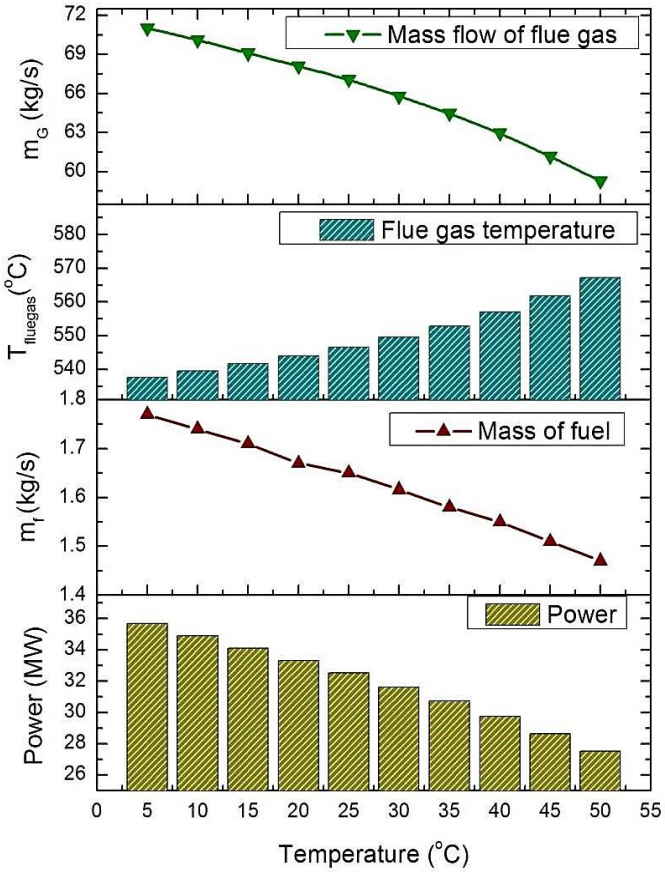

An important element in enhancing the efficiency of a gas turbine cycle is the air intake temperature. Reduced air intake temperature has a significant positive impact on the efficiency of gas turbine power production. On the other hand, a decrease in air intake temperature causes an increase in fuel consumption in order to maintain the required operating temperature at the gas turbine's inlet. Based of the energy balances at the stages of combustion and reheat chambers, the total amount of fuel consumption is calculated. Increased fuel use directly affects the flow rate of exhaust gases. Along with an increase in air intake temperature, the temperature of flue gases released from gas turbines also rises. when a result, ratios of pressure decrease when air intake temperature rises to the desired temperature for gas turbine inlets.

Figure 6 displays the yearly performance of the petrol cycle in terms of energy production and mass of fuel consumption. The air input temperature, as previously mentioned, has a significant impact on how well the gas cycle functions. In the busiest periods of the year, a gas cycle's electrical performance falls by 10%. The winter months have the highest production, at 34 MW. Figure 6 displays the annual fluctuations in the temperatures and production of flue gases. As the pressure ratio decreases at higher air intake temperatures during the summer, the temperature of flue gases increases. Due to lower fuel consumption and air intake rates in the summer, the mass flow rate of the exhaust gases released during the petrol cycle decreases.

IARJSET ISSN (O) 2393-8021, ISSN (P) 2394-1588

International Advanced Research Journal in Science, Engineering and Technology

ISO 3297:2007 Certified ⁜ Impact Factor 8.066 ⁜ Peer-reviewed / Refereed journal ⁜ Vol. 10, Issue 7, July 2023

DOI: 10.17148/IARJSET.2023.10710

Figure 6. Variations in power generation, fuel consumption, and gas cycle exhaust gas characteristics on an annual basis.

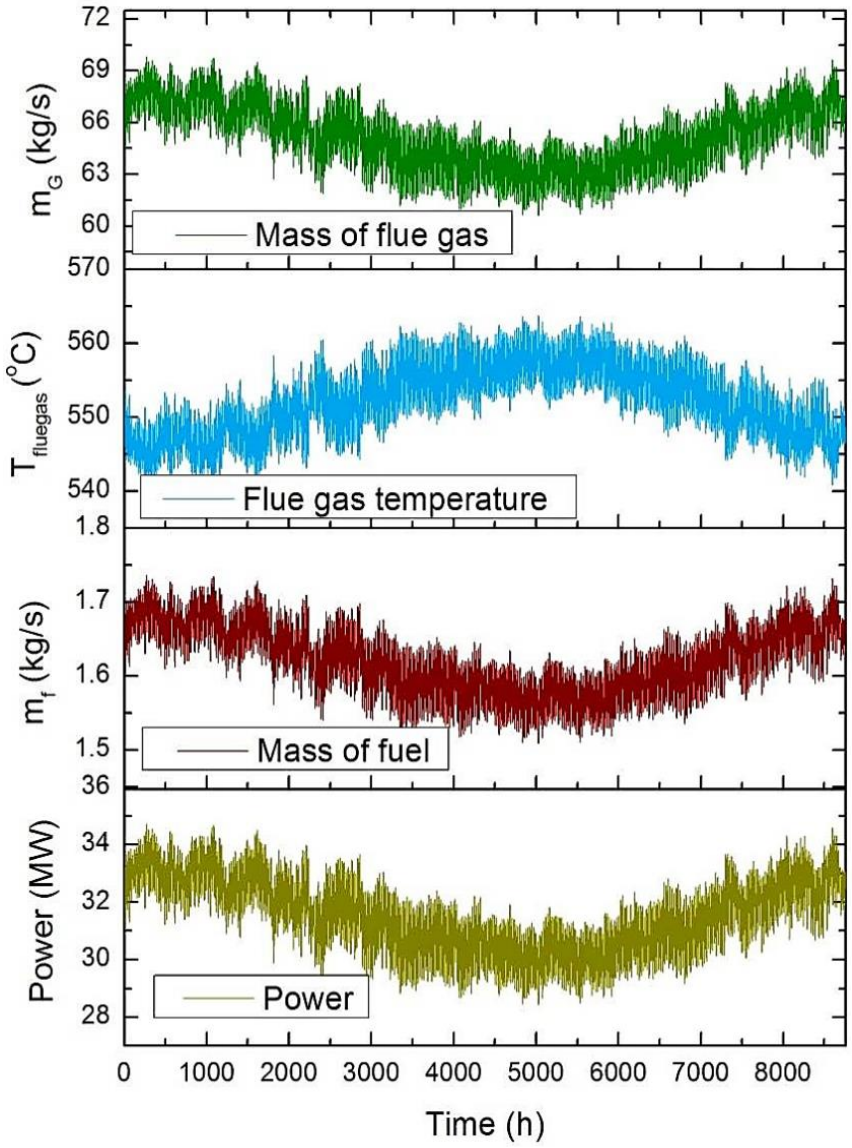

4.2. Steam Cycle

Based on the steam turbine's maximum allowable temperature and pressure ranges, HRSG optimizes the superheated steam's output conditions. For various flue gas intake circumstances, the HRSG system is simulated at a feed pressure of 65 bar. For the safe operation of the steam cycle, feed water flow rates are optimised.

The optimization criteria is to keep the temperature of superheated steam below the steam turbine's maximum permissible temperature limit. The steam cycle's consistent heat recovery can power cooling and desalination cycles all year long by maintaining a steady input water flow rate.

Figure 7 displays the Q-T profile of the HRSG under the design circumstances for the month of July. Simulated HRSG has a pinch point difference of 10 K and a constant approach temperature. The choice of steam turbine depends on the parameters and demands of the design. Table 3 displays the steam turbine's specifications.

IARJSET ISSN (O) 2393-8021, ISSN (P) 2394-1588

International Advanced Research Journal in Science, Engineering and Technology

ISO 3297:2007 Certified ⁜ Impact Factor 8.066 ⁜ Peer-reviewed / Refereed journal ⁜ Vol. 10, Issue 7, July 2023

DOI: 10.17148/IARJSET.2023.10710

Figure 7. *Q-T* profile of HRSG in June.

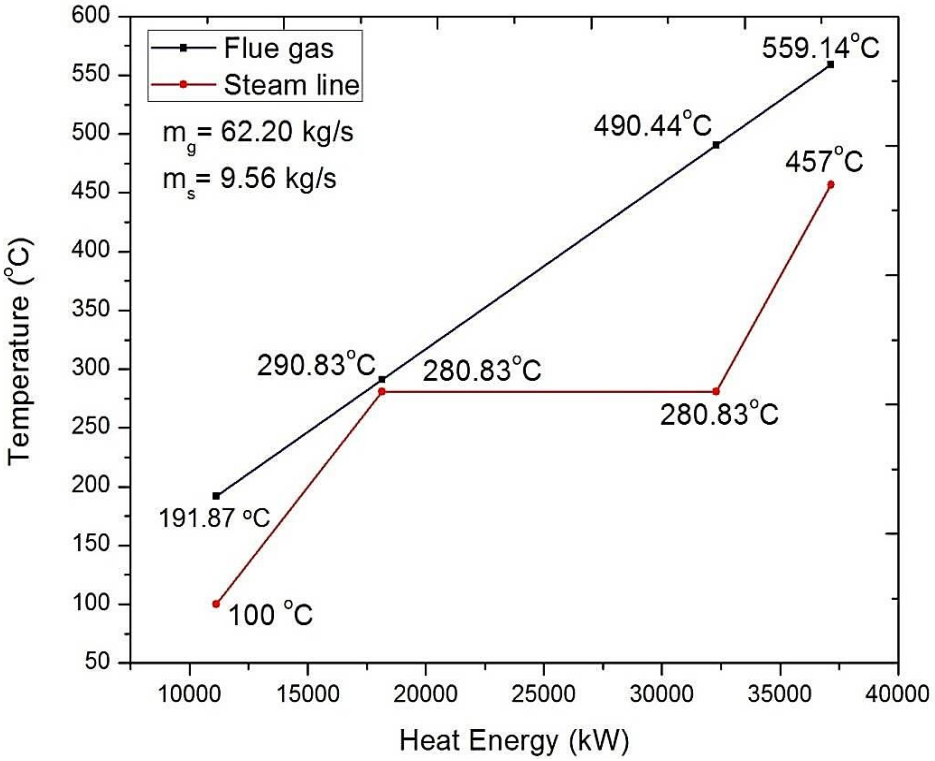

Table 3. Steam turbine technical characteristics [20] Siemens AG, 2014 (Copyright).

No.	Description	Parameters
1	Steam turbine model (Siemens)	SST-100
2	Power output	8.5 MW
3	Inlet steam pressure	Up to 65 bar
4	Inlet steam temperature	Up to 480 °C
5	Condensing pressure	1 bar
6	Exhaust area	0.22 m^2

For fluctuations in air intake temperatures, the functionality of the steam cycle in the tri-generation system is examined. Figure 8a depicts the simulation of the system for various flue gas input conditions. In this study, the primary indicative measures are power generation and stack temperature of flue gases leaving the HRSG.

The steam power cycle produces electricity in a manner similar to a gas power cycle. The main influencing element for the decreasing pattern of power generation is a reduction in the amount of flue gases at increasing air intake temperatures.

The energy balance of the economizer shows that when the mass-flow rate of flue gases falls, so does the stack temperature. Figure 8b depicts the annual performance of the steam cycle. Because of the greater mass-flow rate of flue gases during wintertime months, the functionality of the steam cycle increases.

IARJSET ISSN (O) 2393-8021, ISSN (P) 2394-1588

International Advanced Research Journal in Science, Engineering and Technology

ISO 3297:2007 Certified ⁜ Impact Factor 8.066 ⁜ Peer-reviewed / Refereed journal ⁜ Vol. 10, Issue 7, July 2023

DOI: 10.17148/IARJSET.2023.10710

Figure 8. (**a**) Steam power cycle performance with variable intake temperatures; (**b**) Annual steam cycle performance.

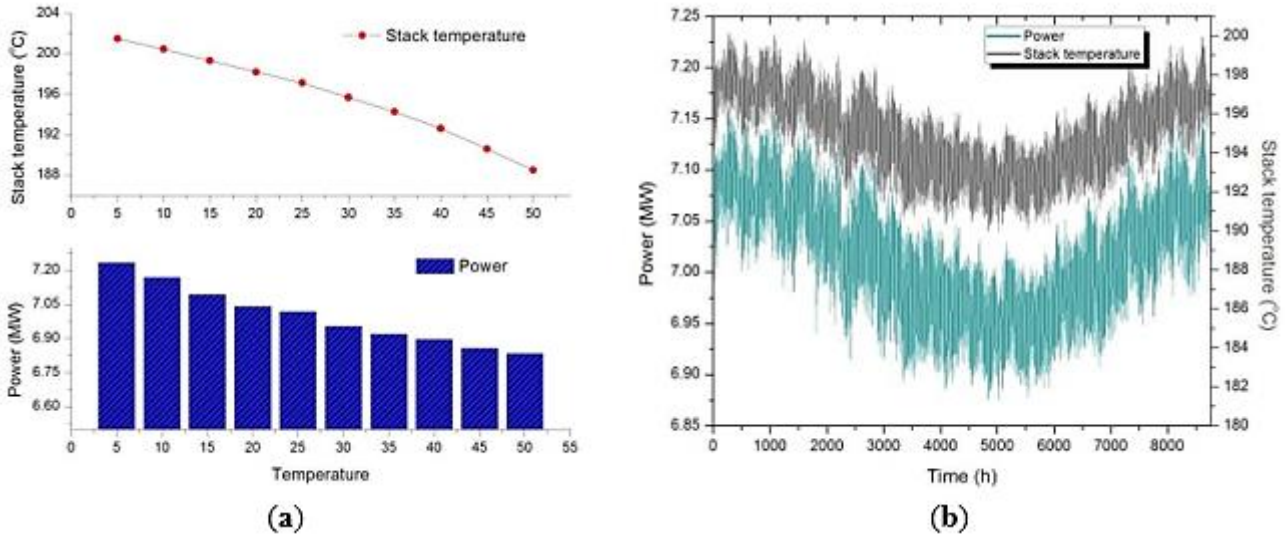

4.3. Absorption Chiller

The regional cooling network takes into account duplex dwellings in the AFAM region. Duplex homes are two identical residences that share a shared wall and have a total floor space of 390 m2 (195 m2 for a single house).

Modelling and simulating the duplex home with TRNBuilt software yields an estimate of the cooling load demand of an ASHRAE-compliant duplex house. Figure 9 depicts the yearly cooling load distribution (hourly distribution) for maintaining an interior set point temperature of 22 °C.

The building simulation is run using a five-person utilization per building and a rate of infiltration of 0.25 ACH. Figure 9 depicts the expanded peak cooling needs of a duplex structure. In the summer, cooling energy demand for a duplex home can reach 36.5 kW; this peak cooling requirement is regarded the design condition for redistribution in the district cooling network. Considering a hot water intake temperature of 90 °C, the chiller's coefficient of performance (COP) ranges between 0.75 and 0.69. The fluctuation in COP is mostly attributable to the temperature of the condenser's cold-water supply.

The overall hot sea water production rate is found to be 358 kg/s based on the energy balances of the heat recovery system. This may be used to calculate the absorption chiller's chilling efficiency. As previously stated, the peak load demand serves as the design criteria for designing the transmission network. Figure 10a depicts the performance of the absorption chiller plant during the peak load interval with varied incoming hot water temperatures.

At higher temperatures, the absorption chiller produces the most cooled energy. At a supply temperature of 90 °C, chilled energy output is 4621.69 kW. It is enough to cover the cooling needs of 124 duplex villas, with a peak cooling demand of 36.5 kW and a COP of 0.69. Reduced input hot water temperature by 10 °C reduces chiller efficiency by 39%; supply temperature drop causes a significant decline in absorption chiller performance.

The absorption chiller's operation is optimised based on what the structure's cooling needs. Figure 10b depicts the absorption chiller's cooling energy generation month by month. The month of June is among the most productive since it coincides with the period of peak cooling energy consumption.

IARJSET ISSN (O) 2393-8021, ISSN (P) 2394-1588

International Advanced Research Journal in Science, Engineering and Technology

ISO 3297:2007 Certified ⁜ Impact Factor 8.066 ⁜ Peer-reviewed / Refereed journal ⁜ Vol. 10, Issue 7, July 2023

DOI: 10.17148/IARJSET.2023.10710

Figure 9. A duplex house's annual cooling load.

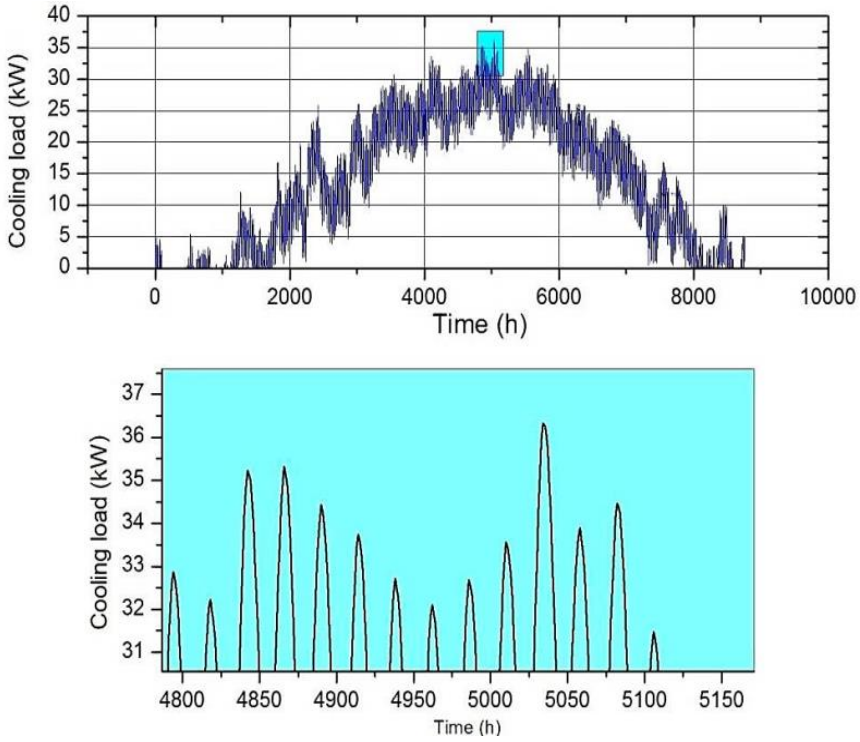

Figure 10. (**a**) Absorption chiller performance with variable intake hot temperature; (**b**) Cooling energy production month by month.

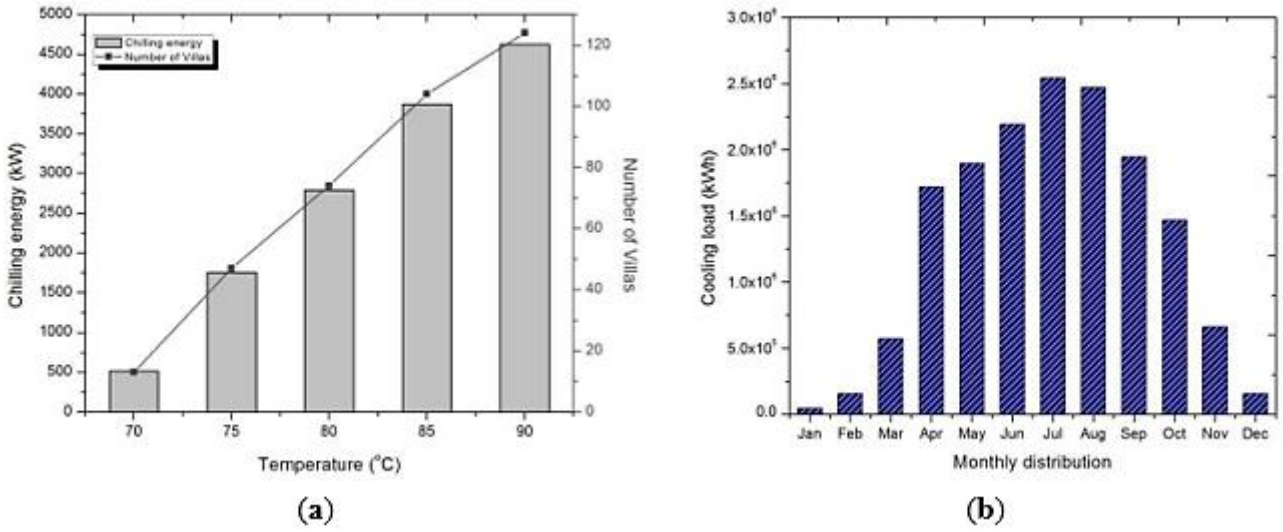

4.4. Membrane Distillation

As illustrated in Figure 10, the functionality of a two phases membrane distillation system is examined by altering the temperatures of the hot and cold sides. Figure 11 depicts the simulation of the system's behaviour for hot side temperatures ranging from 60 to 90 °C and cold side temperatures ranging from 10 to 50 °C with a 5 °C increase.

The productivity of distillate increases as the hot side temperature rises and the chilly side temperature falls. A two phases system's maximum distillate productivity is 41 kg/h with a heated side operating temperature of 90 °C with a chilly side temperature of 10 °C.

IARJSET ISSN (O) 2393-8021, ISSN (P) 2394-1588

International Advanced Research Journal in Science, Engineering and Technology

ISO 3297:2007 Certified ⁜ Impact Factor 8.066 ⁜ Peer-reviewed / Refereed journal ⁜ Vol. 10, Issue 7, July 2023

DOI: 10.17148/IARJSET.2023.10710

Figure 11. Distillate production for temperature variations on the hot and cold sides.

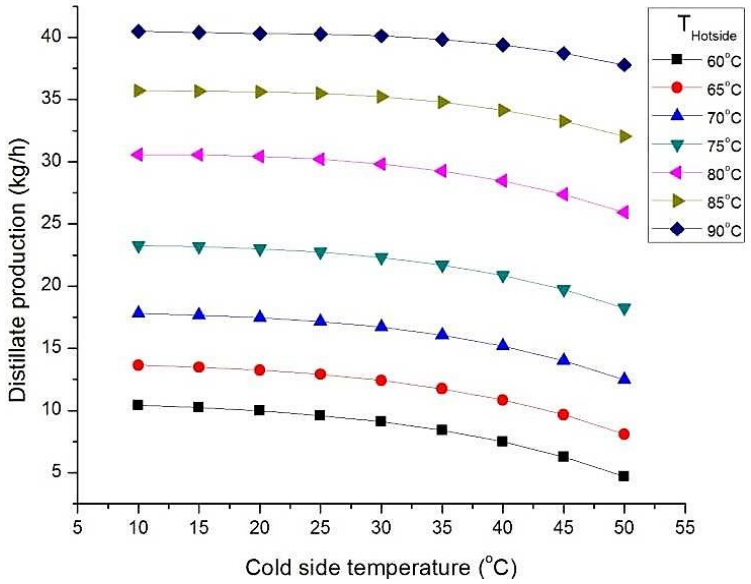

On the basis of the energy balance in the heat recovery system, it is possible to link in parallel a total of 967 multi-effect membrane desalination units, with each unit including two membrane modules connected in series. The membrane distillation plant receives thermal energy that has had its temperature controlled in order to meet the cooling energy needs. The year-round dynamic simulation of a two-stage membrane distillation plant is carried out, and it has been shown that productivity is impacted by both the cold side temperature and the cooling energy needs, as seen in Figures 12 and 13.

The cold side of the membrane distillation system receives supplies of sea water at the temperature that is considered normal. The increasing need for cooling energy and the temperature of the surrounding environment both have a cumulative effect of lowering the desalination plant's overall output. Because of the increased need for cooling energy and the higher temperatures on the cold side, the plant's productivity declines by 12% during the summer months.

Figure 12. The influence that the surrounding temperature has on the distillation process.

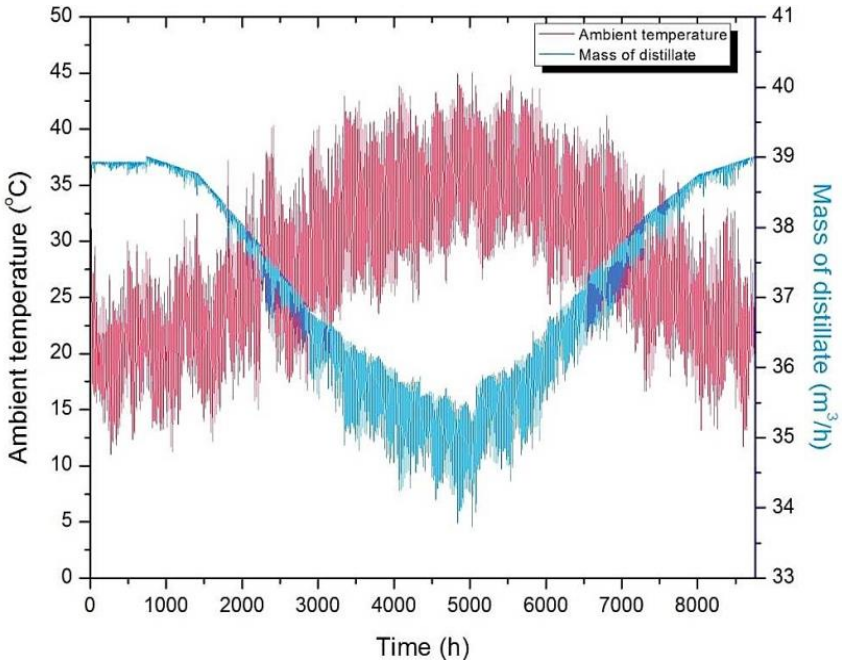

IARJSET ISSN (O) 2393-8021, ISSN (P) 2394-1588

International Advanced Research Journal in Science, Engineering and Technology

ISO 3297:2007 Certified ⁜ Impact Factor 8.066 ⁜ Peer-reviewed / Refereed journal ⁜ Vol. 10, Issue 7, July 2023

DOI: 10.17148/IARJSET.2023.10710

Figure 13. The influence of cooling load on the generation of distillate.

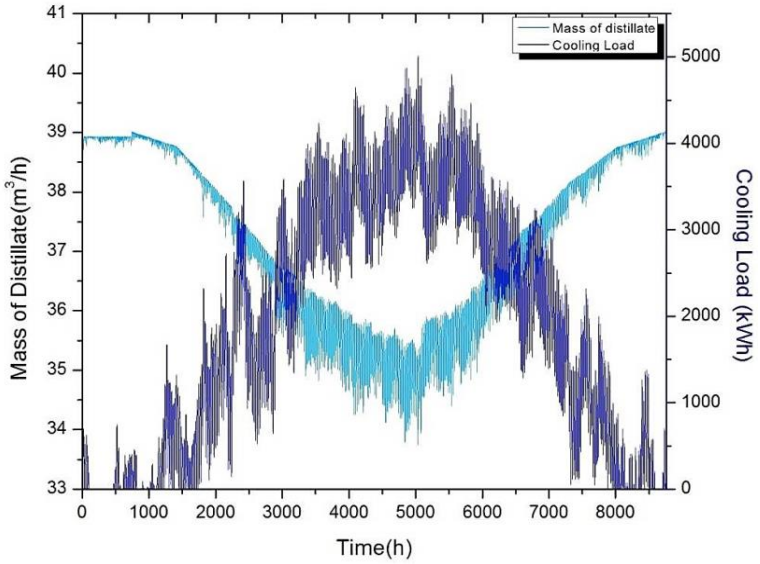

4.5. Energy Efficiency

Month-wise energy distribution between different thermal cycles of the tri-generation system is shown in Figure 14a. Useful energy produced by the tri-generation cycle is reduced in the summer months due to higher air intake temperature in the gas cycle leading to lesser fuel consumption. Month-wise energy efficiencies of gas cycle, combined cycle and tri-generation cycle is shown in Figure 14b. The gas cycle efficiency and combined cycle efficiency reduces in summer months due to lower power production, while the efficiency of tri-generation cycle increases by 4% during this period due to full scale operation of absorption chiller plant as shown in Figure 14b.

Figure 14. (**a**) Distribution of energy according to the months; (**b**) Distribution of cycle efficiencies on an annual basis.

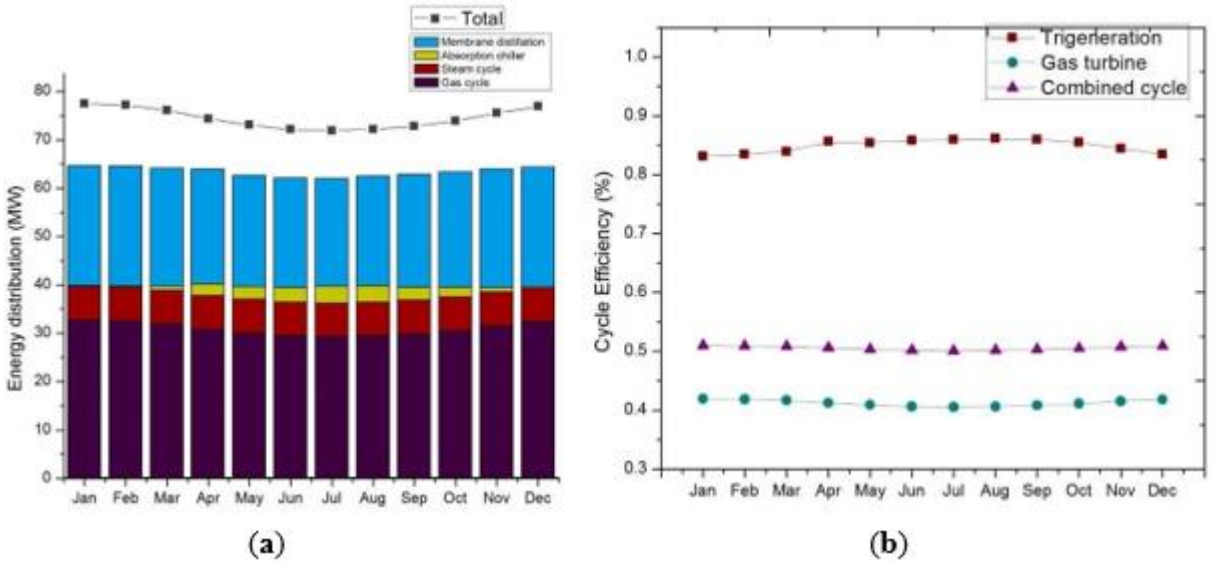

Figure 15 is a sankey diagram that represents the flow of energy at peak load circumstances. Problems with sulphur condensation prevented the recovery of approximately one quarter of the waste heat; nonetheless, the vast majority of the waste heat was put to use in the manufacture of water that was clean.

IARJSET ISSN (O) 2393-8021, ISSN (P) 2394-1588

International Advanced Research Journal in Science, Engineering and Technology

ISO 3297:2007 Certified ⁜ Impact Factor 8.066 ⁜ Peer-reviewed / Refereed journal ⁜ Vol. 10, Issue 7, July 2023

DOI: 10.17148/IARJSET.2023.10710

Figure 15. Sankey diagram of energy flows.

portable devices.

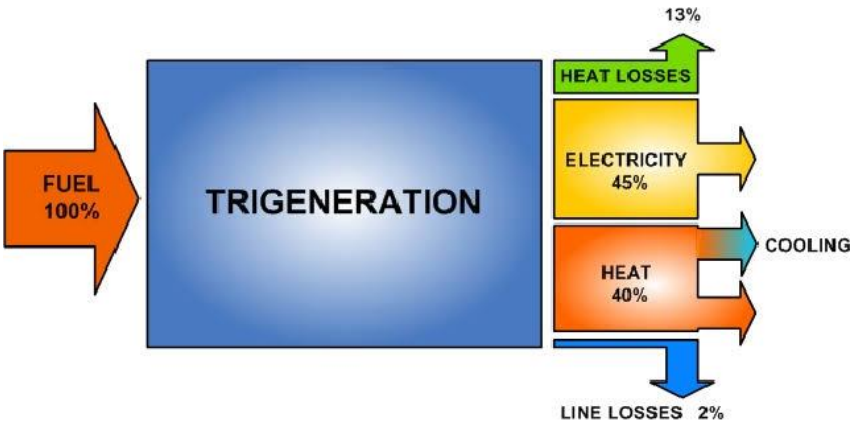

4.6. Emission Analysis

In addition to the energy gains that come in the form of high thermal efficiency, there is also the possibility that the tri-generation system may cut down on emissions of greenhouse gases. The implementation of poly-generation cycles results in a reduction in the normalised emission of CO2 and NOx per MWh. Figure 16 depicts the varying levels of emissions produced by each of the three cycles (the gas cycle, the combined power cycle, and the tri-generation cycle). When calculating CO2 emissions on a yearly scale, the CO2 coefficient emission per kWh of energy output is the metric that is utilised. The CO2 emission coefficient for NIGERIA is 600 g of CO2 per kWh of energy output [21]. The fact that the tri-generation system has a 51.5% reduction in its normalised CO2 emissions demonstrates that the system is environmentally sustainable. This decrease in normalised CO2 emissions is accomplished by the avoidance of total CO2 by running the tri-generation system with recovered waste heat. In the case of trigeneration, production has grown by 51.5% while consuming the same quantity of fuel, which has resulted in reduced levels of carbon emission. In addition to CO2 emissions, other greenhouse gas emissions such as NOx and SOx saw a 51.5% decrease. NOx emissions account for 5% of the country's overall GHG output, which results in a normalised production of 38 g of CO2 equivalents per kWh [22]. The use of trigeneration results in a reduction in NOx emissions to 18.4 g per kWh. The current gas turbine power plant is responsible for an estimated amount of total CO2 and NOx emissions:

$$Total\ emissions = emission\ coefficient \times Annual\ electricity\ production \qquad (30)$$

Figure 16. CO2 and NOx emissions after normalization.

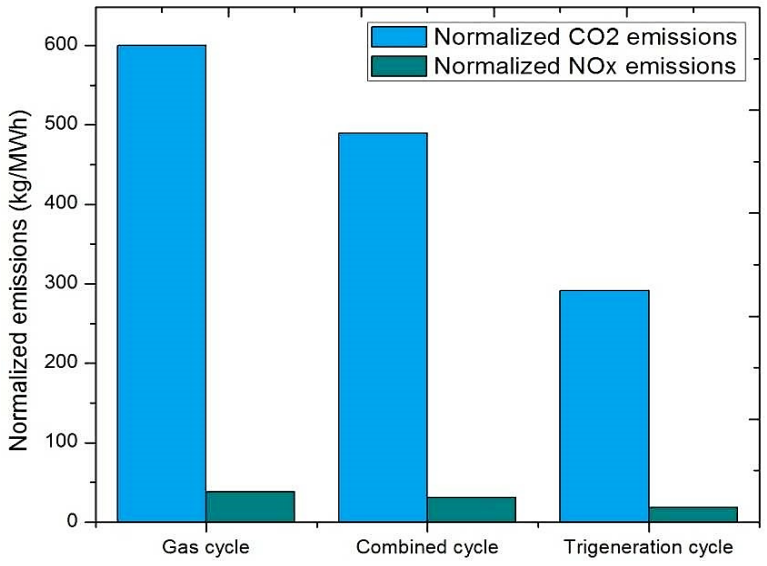

IARJSET ISSN (O) 2393-8021, ISSN (P) 2394-1588

International Advanced Research Journal in Science, Engineering and Technology

ISO 3297:2007 Certified ⁜ Impact Factor 8.066 ⁜ Peer-reviewed / Refereed journal ⁜ Vol. 10, Issue 7, July 2023

DOI: 10.17148/IARJSET.2023.10710

4.7. Economic Analysis

In this part, we will analyse the economic benefits of adopting a tri-generation system for the recovery of waste heat. As a result of the use of waste heat in the overall operation, the tri-generation system is able to achieve significantly reduced operating costs. Table 4 provides an overview of the prices of the different components as well as other relevant factors. Table 5 presents an estimation of the total investment, operation and maintenance expenses, and yearly benefits.

Table 4. Economic analysis requires parameters and costs.

Component	Abbreviation	Value
Heat recovery steam generator [23]	C_{HRSG}	Equation (33)
Steam turbine [23]	C_{ST}	Equation (37)
Heat recovery unit [24]	C_{HRS}	$2,000/m^2
Feed water pump (Steam cycle) [25]	$C_{ST.PUMP}$	$881W_{p0.4}$
Membrane distillation unit [26]	C_{AGMD}	$1,375/unit
Membrane replacement cost [24]	$C_{MD.R}$	15% of C_{AGMD}
Feed pump (Heat recovery) [25]	$C_{HRS.PUMP}$	$881W_{p0.4}$
Absorption chiller [27]	C_{AC}	$400/kW
Hydraulics [26]	C_{HYD}	5% of component costs
Installation cost [26]	C_I	5% of component costs
Interest rate	i	10%
Life time of the project	n	20 years
Cost of electricity	C_F	$0.12/kW·h

Table 5. Economic evaluation of a trigeneration system.

No.	Parameters	Values
1	Investment cost	$11,079,548
2	Operating and maintenance cost	$443,494
3	Annual benefits	$9,413,460
4	Payback period	1.38 years
5	Net present value	$66,102,281

Table 5 presents the findings of an analysis conducted on the cumulative net present value (NPV) and payback period (PB) of the tri-generation system. The anticipated yearly advantages of installing trigeneration are based on the total annual output of power, cooling, and freshwater, as indicated in Table 6. We may estimate the project's net present value by using the following formulas:

$$NPV = -C_0 + (B - C)\left[\frac{(1+i)^n - 1}{i(1+i)^n}\right] \quad (31)$$

wherein CI is the total amount of investing, B is the yearly benefits, C is the annual cost of maintenance and operation, i is the rate of return on investment, and n is the number of years the project will be in operation. The following factors will affect how long it will take for the project to break even:

$$PB = \frac{\ln(B - C) - \ln[(B - C) - iC_0]}{\ln(1 + i)} \quad (32)$$

IARJSET ISSN (O) 2393-8021, ISSN (P) 2394-1588

International Advanced Research Journal in Science, Engineering and Technology

ISO 3297:2007 Certified ⁜ Impact Factor 8.066 ⁜ Peer-reviewed / Refereed journal ⁜ Vol. 10, Issue 7, July 2023

DOI: 10.17148/IARJSET.2023.10710

[23] determines the investment in HRSG and steam turbine:

$$C_{\mathrm{HRSG}} = 4131.8\left(f_{\mathrm{p}}.f_{\mathrm{T,steam}}.f_{\mathrm{T,gas}}\left(\frac{Q}{\Lambda\, T_{\mathrm{ln}}}\right)^{0.8}\right) + 13380\left(f_{\mathrm{p}}.\dot{m}_{\mathrm{steam}}\right) + 1489.7\dot{m}_{\mathrm{gas}}^{1.2} \quad (33)$$

$$f_{\mathrm{p}} = 0.0971\frac{Pr}{30\ bar} + 0.9029 \quad (34)$$

$$f_{\mathrm{T,steam}} = 1 + exp\left(\frac{T_{\mathrm{out,steam}} - 830}{500}\right) \quad (35)$$

$$f_{\mathrm{T,gas}} = 1 + exp\left(\frac{T_{\mathrm{out,gas}} - 990}{500}\right) \quad (36)$$

$$C_{\mathrm{ST}} = 3880.5P_{\mathrm{ST}}^{0.7}\left(1 + \left(\frac{0.05}{1-\eta_{\mathrm{ST}}}\right)^{3}\right).\left(1 + 5exp\left(\frac{T_{\mathrm{in}} - 866}{10.52}\right)\right) \quad (37)$$

wherein Q is the amount of heat transfer within the HRSG, Tln is the temperature differential across the HRSG, and Pr is the pressure of feed water to the HRSG. Calculating the overall investment cost (CO) of the project includes the following steps:

$$C_{\mathrm{O}} = C_{\mathrm{HRSG}}(P_{\mathrm{HRSG}}) + C_{\mathrm{ST}}(P_{\mathrm{ST}}) + C_{\mathrm{HRS}}(A_{\mathrm{HRS}}) + C_{\mathrm{ST,PUMP}}(P_{\mathrm{ST,PUMP}}) + C_{\mathrm{AGMD}}(N_{\mathrm{AGMD}}) + C_{\mathrm{HRS,PUMP}}(P_{\mathrm{HRS,PUMP}}) + C_{\mathrm{AC}}(P_{\mathrm{AC}}) + C_{\mathrm{HYD}} \quad (38)$$

, as well as represent the combined capacities of the heat recovery system (HRSG), steam turbine (ST), and feed pumps (feed pumps) in the steam cycle. AHRS is the area of the heat recovery system, while NAGMD is the total amount of the membrane distillation modules. The power needs for the feed pumps and the membrane replacement charges are included in the yearly maintenance and operation cost for the tri-generation plant.

Table 6. Annual benefits.

Parameters	Value	Total benefits
Electricity production	$0.12/kW·h	$7,289,423.73
Cooling benefits	$0.10/kW·h	$1,582,854.46
Cooling demand charges	$42.3/kW·year	$211,500.00
Water production cost	$1/m³	$329,681.90

Figure 17 depicts the proportion of the overall investment that is attributable to the various expenses of the equipment. The membrane of the distillation unit and the steam turbine together contribute to close to 46% of the entire cost of investment.

The payback time for the system is only 1.38 years, and it has a bigger cumulative profit of $66.10 million. This is based on the current cost of gasoline in the area. Figure 18 depicts an economic analysis taking into account the likelihood of fluctuations in the cost of power. Figure 19 depicts the results of a simulation that applies a 10% interest rate to the annual cash flows generated by the project. When the current worth element is taken into account, the cash flow gets lower as the number of years increases.

IARJSET ISSN (O) 2393-8021, ISSN (P) 2394-1588

International Advanced Research Journal in Science, Engineering and Technology

ISO 3297:2007 Certified ⁜ Impact Factor 8.066 ⁜ Peer-reviewed / Refereed journal ⁜ Vol. 10, Issue 7, July 2023

DOI: 10.17148/IARJSET.2023.10710

Figure 17. Cost sharing across many investments.

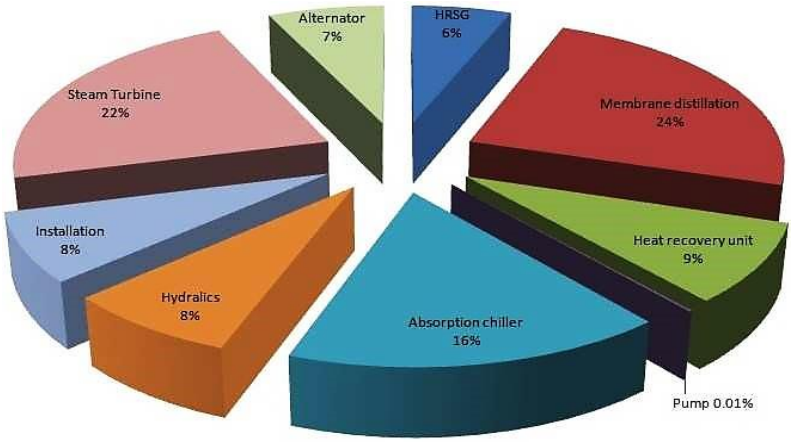

Figure 18. Evaluation of the economy concerning the three-generation system.

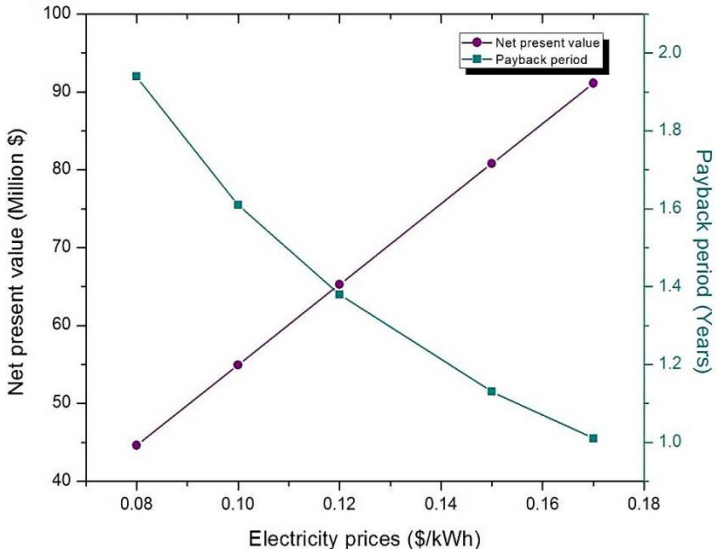

Figure 19. Trigeneration system cash flows.

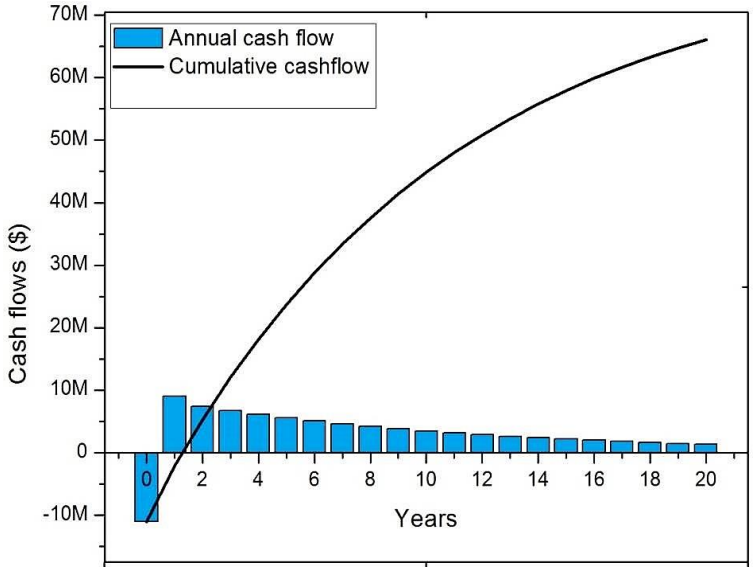

IARJSET ISSN (O) 2393-8021, ISSN (P) 2394-1588

International Advanced Research Journal in Science, Engineering and Technology

ISO 3297:2007 Certified ⁜ Impact Factor 8.066 ⁜ Peer-reviewed / Refereed journal ⁜ Vol. 10, Issue 7, July 2023

DOI: 10.17148/IARJSET.2023.10710

Figure 20: Air Gap Membrane distillation plants

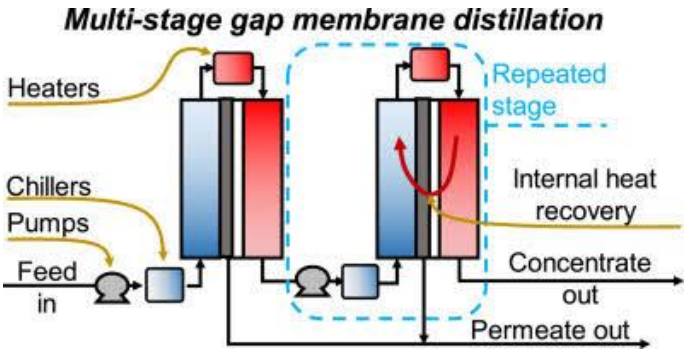

Figure 21: Single stage air gap membrane distillation

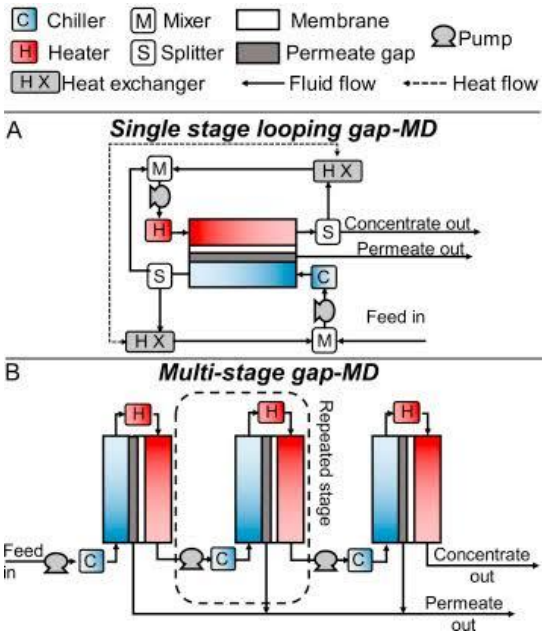

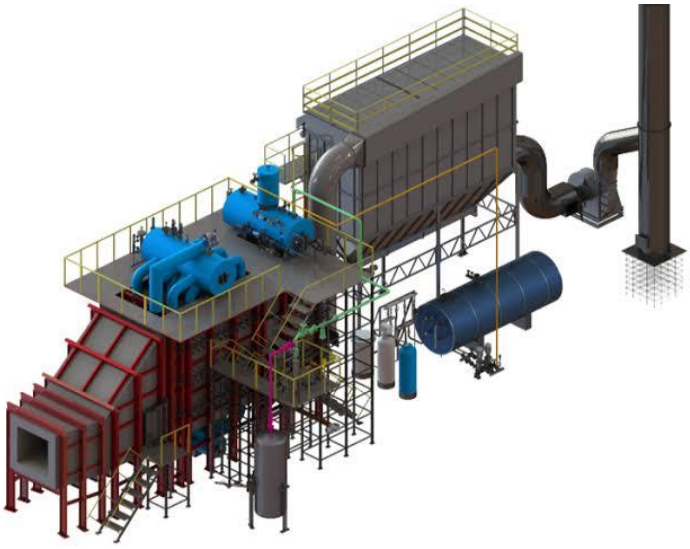

IARJSET ISSN (O) 2393-8021, ISSN (P) 2394-1588

International Advanced Research Journal in Science, Engineering and Technology

ISO 3297:2007 Certified ⁜ Impact Factor 8.066 ⁜ Peer-reviewed / Refereed journal ⁜ Vol. 10, Issue 7, July 2023

DOI: 10.17148/IARJSET.2023.10710

Figure 22: HRSG/WT -water tube, waste Heat steam

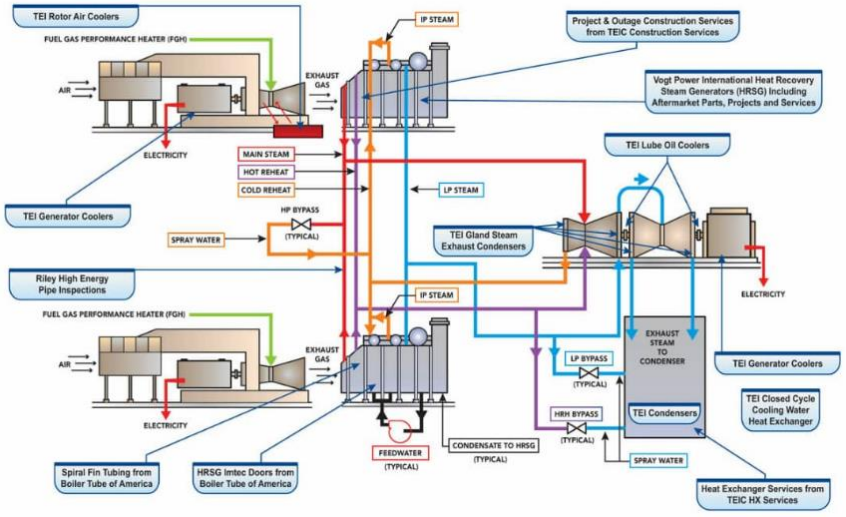

Figure 23: Overview of Combine cycle plant

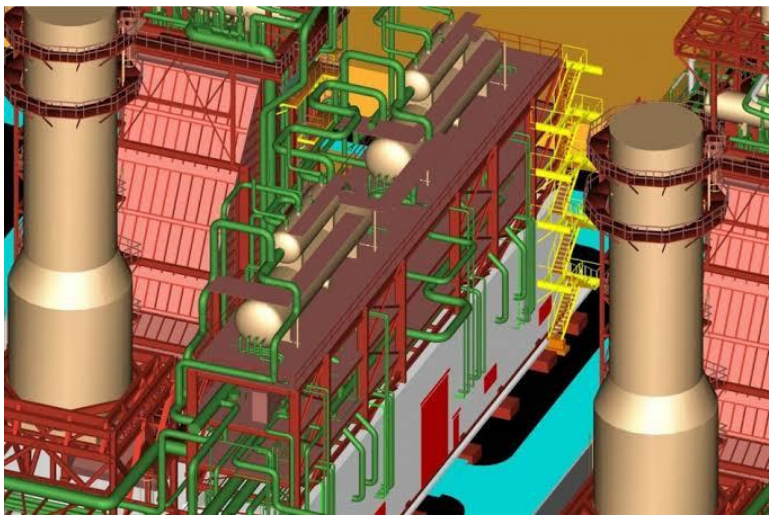

Figure 24: Piping Engineering of Heat Recovery steam generator unit

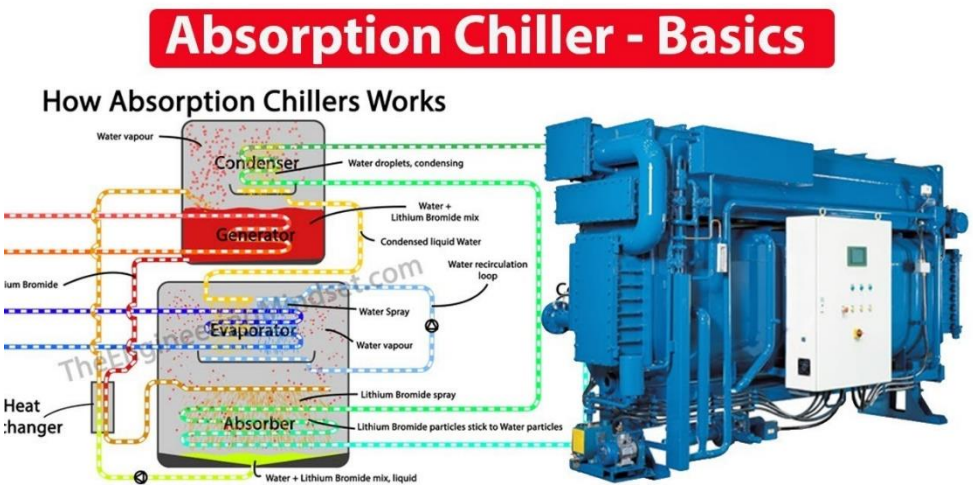

IARJSET ISSN (O) 2393-8021, ISSN (P) 2394-1588

International Advanced Research Journal in Science, Engineering and Technology

ISO 3297:2007 Certified ⁜ Impact Factor 8.066 ⁜ Peer-reviewed / Refereed journal ⁜ Vol. 10, Issue 7, July 2023

DOI: 10.17148/IARJSET.2023.10710

Figure 25: Vapor absorption chiller

Figure 26: Modular HRGS

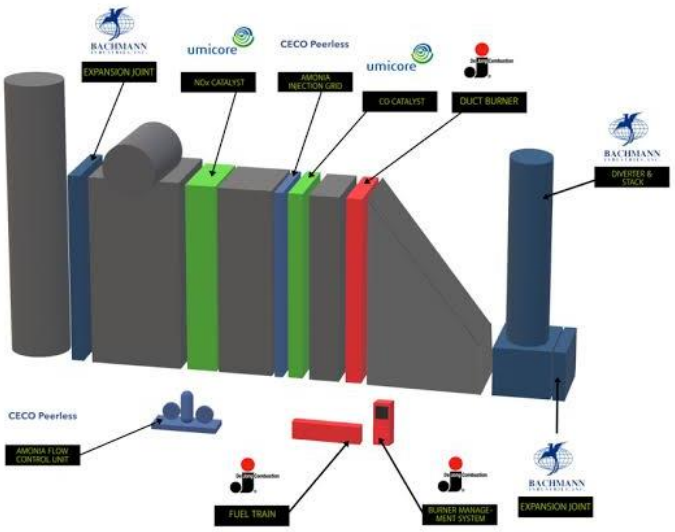

Figure 27: Emission control system

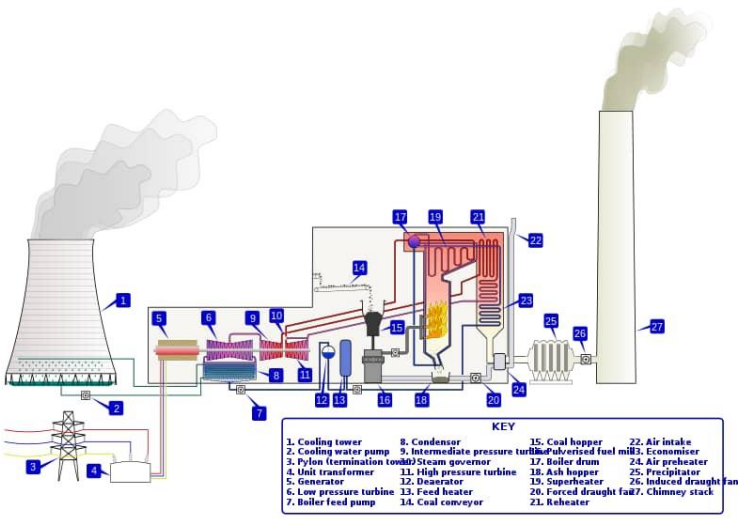

IARJSET ISSN (O) 2393-8021, ISSN (P) 2394-1588

International Advanced Research Journal in Science, Engineering and Technology

ISO 3297:2007 Certified ⁜ Impact Factor 8.066 ⁜ Peer-reviewed / Refereed journal ⁜ Vol. 10, Issue 7, July 2023

DOI: 10.17148/IARJSET.2023.10710

Figure 28: Steam cycle power plant

V. CONCLUSIONS

The combination of power, cooling, with desalination thermal cycles formed the basis for the presentation of a tri-generational system. The implementation of the project in the Afam region of Rivers state in Nigeria, prompted the development of a comprehensive numerical case study. The mathematical representation of the trigenerational system is designed to make the most efficient use of wasted heat by driving four different thermal cycles, each of which is determined by the quality and degree Celsius of the thermal energy being generated. The performance of the absorption chiller plant has been fine-tuned to meet the cooling energy demands of duplex villas located in the region. The findings of the simulation reveal that the energetic efficiency of the tri-generation system may be maximised by up to 85% during the summer months due to decreased fuel usage and the operation of the absorption chiller at full size. The air intake temperature has a significant impact on the performance of the thermal cycle; however, because the need for cooling is less in the winter, the total thermal efficiency decreases as the air intake temperature drops. The following is a list of further significant insights gained from the initiative of recovering waste heat from current energy plants:

- The system has a quick payback time of 1.38 years and a cumulative savings of $66 million, which makes it economically advantageous.
- The output capacity of a membrane distillation plant can range from 33 to 37 m3/h depending on the daily cooling requirements and the temperature of the surrounding environment;
- The deployment of the waste heat recovery system results in a reduction in the normalised CO2 emission per MWh from an actual scenario of 600 kg/MWh to 291 kg/MWh; this is a reduction of 39%;
- The absorption chiller system has the potential to supply district cooling for 124 duplex houses at times of peak demand, giving it a production capacity of 4600 kW;

ACKNOWLEDGMENT:

The authors would like to express their gratitude to the researchers and academics who have made important, trustworthy, and accurate material on all areas of Gas Turbine, Heat Recovery Steam Generation, steam cycle power plant, And Tri-generation readily available. This contributed to the overall success of the study's development.

CONFLICTS OF INTEREST:

The Authors declare that they have no conflict of interest.

AUTHORS CONTRIBUTION:

The first author wrote the draft under the guidance of the second author on the theme and content of the paper.

FUNDING STATEMENT:

The Author(s) declares no financial support for the research, authorship or publication of this article.

DOI: 10.17148/IARJSET.2023.10710

REFERENCES

[1] Kong, X.Q.; Wang, R.Z.; Huang, X.H. Energy optimization model for a CCHP system with available gas turbines. *Appl. Therm. Eng.* **2005**, *80*, 377–391.
[2] Khan, K.H.; Rasul, M.G.; Khan, M.M.K. Energy conservation in buildings: Cogeneration and cogeneration coupled with thermal-energy storage. *Appl. Therm. Eng.* **2004**, *77*, 15–34.
[3] Havelsky, V. Energetic efficiency of cogeneration system for combined heat, cold and power production. *Int. J. Refrig.* **1999**, *22*, 479–485.
[4] Bilgen, E. Exergetic and engineering analyses of gas turbine-based cogeneration systems. *Energy* **2000**, *25*, 1215–1229.
[5] Huangfu, Y.; Wu, J.Y.; Wang, R.Z.; Kong, X.Q.; Wei, B.H. Evaluation and analysis of novel micro-scale combined cooling, heating and power (MCCHP) system. *Energy Convers. Manag.* **2007**, *48*, 1703–1709.
[6] Liu, M.; Shi, Y.; Fang, F. Combined cooling, heating and power systems: A survey. *Renew. Sustain. Energy Rev.* **2014**, *35*, 1–22.
[7] Ahmadi, P.; Dincer, I.; Rosen, M.A. Exergo-environmental analysis of an integrated organic Rankine cycle for trigeneration. *Energy Convers. Manag.* **2012**, *64*, 447–453.
[8] Khaliq, A. Exergy analysis of gas turbine trigeneration system for combined production of power heat and refrigeration. *Int. J. Refrig.* **2009**, *32*, 534–545.
[9] Ahmadi, P.; Rosen, M.A.; Dincer, I. Greenhouse gas emission and exergo-environmental analyses of a trigeneration energy system. *Int. J. Greenh. Gas Control* **2011**, *5*, 1540–1549.
[10] Temir, G.; Bilge, D. Thermoeconomic analysis of a trigeneration system. *Appl. Therm. Eng.* **2004**, *24*, 2689–2699.
[11] Sun, Z.G. Energy efficiency and economic feasibility analysis of cogeneration system driven by gas engine. *Energy Build.* **2008**, *40*, 126–130.
[12] Hussain, H.J. Development of a Hybrid Powerplant for Kuwait: The Simultaneous Production of Power, Fresh Water and Cooling. Ph.D. Thesis, Cranfield University, Shrivenham, UK, 2010.
[13] Calise, F.; d'Accadia, M.D.; Piacentino, A. A novel solar trigeneration system integrating PVT (photovoltaic/thermal collectors) and SW (Seawater) desalination: Dynamic simulation and economic assessment. *Energy* **2014**, *67*, 129–148.
[14] Kullab, A.; Martin, A. Membrane distillation and applications for water purification in thermal cogeneration plants. *Sep. Purif. Technol.* **2011**, *76*, 231–237.
[15] Liu, C. Polygeneration of Electricity, Heat and Ultrapure Water for the Semiconductor Industry. Master's Thesis, KTH Royal Institute of Technology, Stockholm, Sweden, 2004.
[16] Kullab, A. Desalination using Membrane Distillation: Experimental and Numerical study. Ph.D. Thesis, KTH Royal Institute of Technology, Stockholm, Sweden, 2011.
[17] Burrieza, E.G.; Blanco, J.; Zaragoza, G.; Alarcón, D.C.; Palenzuela, P.; Ibarra, M.; Gerjak, W.
Experimental analysis of an air gap membrane distillation solar desalination pilot plant system. *J. Membr. Sci.* **2011**, *379*, 386–396.
[18] RAK Property Services. Available online: http://www.rakps.com (accessed on 2 June 2014).
[19] *Data Sheet of Test Results—GE Energy*; Al-Hamra Gas Turbine Powerplant: Ras Al Khaimah, UAE. Unpublished work, 2014.
[20] Technical Specification of Steam Turbine SST-100. Available online: http://www.energy.siemens.com (accessed on 25 April 2014).
[21] International Energy Agency (IEA) STATISTICS 2012. CO_2 Emissions from Fuel Combustion. Available online: http://www.iea.org (accessed on 5 May 2014).
[22] *Greenhouse Gas Inventory for Abu Dhabi Emirate: Inventory Results Executive Summary*; Environment Agency—Abu Dhabi: Abu Dhabi, UAE, 2012.
[23] Roosen, P.; Uhlenbruck, S.; Lucas, K. Pareto optimization of a combined cycle power system as a decision support tool for trading off investment *vs.* operating cost. *Int. J. Therm. Sci.* **2003**, *42*, 553–560.
[24] Al-Obaidani, S.; Curcio, E.; Macedonio, F.; Profio, G.D.; Al-Hinai, H.; Drioli, E. Potential of membrane distillation in seawater desalination: Thermal efficiency, sensitivity and cost estimation. *J. Membr. Sci.* **2008**, *323*, 85–98.
[25] Alili, A.A.; Islam, M.D.; Kubo, I.; Hwang, Y.; Radermacher, R. Modeling of a solar powered absorption cycle for Abu Dhabi. *Appl. Energy* **2012**, *93*, 160–167.
[26] *Performance and Cost Estimations of Final Industrial Size of MEDESOL-2 Technology 2010*; University of La Laguna: Canary Islands, Spain, 2010.
[27] Lazzarin, R.M. Solar cooling: PV or thermal? A thermodynamic and economic analysis. *Int. J. Refrig.* **2014**, *39*, 38–47. 2014 by the authors; licensee MDPI, Basel, Switzerland. This article is an open access article distributed under the terms and conditions of the Creative Commons Attribution license (http://creativecommons.org/licenses/by/4.0/).